

DOI: <http://dx.doi.org/10.21123/bsj.2021.18.2.0401>

Cobalt Effect on the Growth of Cadmium Oxide Nanostructure Prepared by Spray Pyrolysis Technique

Jamal M. Rzaij^{1*}

A. S. Ibraheem²

Amina M. Abass³

¹Department of Physics, College of Science, University of Anbar, Ramadi, Iraq

²Iraqi Ministry of Education, Anbar, Iraq.

³Department of Chemistry, College of Science, Al-Nahrain University, Baghdad, Iraq

*Corresponding author: sc.jam72al@uoanbar.edu.iq, auth_1982@yahoo.com, aminamohsen75@gmail.com

*ORCID ID: <https://orcid.org/0000-0003-2287-3083>, <https://orcid.org/0000-0003-4882-1134>, <https://orcid.org/0000-0003-3043-9076>

Received 25/10/2019, Accepted 10/6/2020, Published Online First 11/1/2021



This work is licensed under a [Creative Commons Attribution 4.0 International License](https://creativecommons.org/licenses/by/4.0/).

Abstract:

Spray pyrolysis technique (SPT) is employed to synthesize cadmium oxide nanostructure with 3% and 5% Cobalt concentrations. Films are deposited on a glass substrate at 350 °C with 150 nm thickness. The XRD analysis revealed a polycrystalline nature with cubic structure and (111) preferred orientation. Structural parameters represent lattice spacing, crystallite size, lattice parameter and dislocation density. Homogeneous surfaces and regular distribution of atoms were showed by atomic force microscope (AFM) with 1.03 nm average roughness and 1.22 nm root mean square roughness. Optical properties illustrated a high transmittance more than 85% in the range of visible spectrum and decreased with Co concentration increasing. The absorption coefficient values decreased with increasing wavelength and the prepared films had absorption coefficient values greater than 10^4 cm^{-1} . The optical energy gap values for allowing direct transition (ADT) varied from 2.78 to 2.63 eV with increasing Co concentration, while the energy gap for allowing indirect transition (AIDT) varied from 1.85 to 1.6 eV with Co concentration.

Key words: Cadmium oxide, Cobalt, Optical properties, Spray pyrolysis, Thin films.

Introduction:

TCOs or transparent conducting oxides are compounds that either have a binary or ternary compound. They are unique materials because they show the transparency of light and electrical conductivity at the same time, therefore, they are a fundamental pillar in the study of the properties of physical substances as well as their adoption in many applications (1). To examine the physical properties of the material, they must be chosen so that they could possess adequate large energy gap to be transparent to visible type of light, which cannot be absorbed, as well as the high concentration of holes and/or electrons, electrical conductivity, that maintain a good mobility (2). Glass fibers are considered transparent material, but are classified as insulators while semiconductors are materials that adopt the doping with metal elements to be able to the electrical conductivity. Therefore, the transparent conductive oxides embrace the two contradicting properties so that their electrical conductivity can be close to the metals in addition

to the high transparency of light (3,4). TCOs are compound semiconductors made of metal combined with oxygen. This material possesses high optical conductivity within the spectrum region extending from 400 nm to 1500 nm, despite the widening energy gap of these materials, but the conduction band is filled with free electrons due to the high concentration of charge carriers (5,6). Several previous studies dealt with the study of transparent conducting oxides and their physical fundamentals in addition to their structural properties (6–8)

Examples of binary and ternary TCOs are CdO, ZnO, In_2O_3 , SnO_2 , Ga_2O_3 , Cd_2SnO_4 , CdSnO_3 , Zn_2SnO_4 and CdIn_2O_4 . Cadmium oxide is one of the most important of these oxides because it has optical energy gap ranging from 2.18 to 2.31 eV at room temperature (2), as well as high transparency of light within the range of the visible spectrum of electromagnetic radiation. It is considered as one of the promising materials in the use of many applications such as solar cells, photodiodes, gas

sensors, light detectors, liquid crystal displays, and other applications that fall into the daily life (9). In literature review, several methods were used to prepare cadmium oxide thin films. In 1987, B. Kavitha *et al.* (10) developed thin films of CdO on glass substrate at 70°C using the successive ionic layer adsorption and reaction (SILAR). Usharani *et al.* (7) explored the possibility using cadmium oxide thin films in optical applications using the spray pyrolysis technique and the effect of substrate temperature on the optical and structural properties of these films on a glass substrate in 2015. In 2017, M. R. DAS *et al.* (11) assessed the effect of deposition time on the structural and electrical properties of cadmium oxide thin films on a glass substrate using chemical bath deposition technique (CBD). A. A. Shehab *et al.* (12) in 2012, studied the effect of tin doping on some physical properties of CdO thin films prepared by thermal vacuum evaporation (PVD) method at 300K with 400 nm thickness. Using reactive magnetron sputtering P. Dhivya *et al.* (13) prepared thin films of CdO in 2012 at room temperature for sensing the hydrogen gas after annealing the samples at various temperatures. The best results in response to the gas sensor, are given by the sample annealed at 100°C. In 1999, and by using the cadmium chloride solution, M. D. Uplane *et al.* (14) investigated thin films of CdO using a spray pyrolysis technique with polycrystalline structure. A direct energy gap of 1.9 eV was obtained. Non-transparent CdO films were obtained by J. G. Quinones *et al.* (15) (2016) using pulsed laser deposition (PLD). Structural analysis showed that the films were crystallized after being heat treated with a temperature of 500°C. Electrical properties indicated an increase in the electrical resistance for thermally annealed samples compared to non-annealed samples.

The purpose of this work is to prepare nanocrystalline thin films of cadmium oxide compound undoped and doped with different concentrations of cobalt using the spray pyrolysis simple and inexpensive technique. Doping effect on the structural, morphological and optical properties such as transmission, absorption coefficient, direct

and indirect energy gap and finding the limitation of using these films in different optoelectronic applications is the main thrust of this work.

Materials and Methods:

Cadmium nitrate tetrahydrate, Cd(NO₃)₂.4H₂O, (BDH Chemical England, 99.5% purity), a white powder that is soluble in water used for the preparation of un-doped CdO thin films. The solution was prepared with a concentration of 0.1M according to relation (1). The weight of the material was calculated using a sensitive electronic balance (Mettler HK-160 with 10⁻⁴ g sensitivity). The material was added to 100 ml of distilled water, then gradually dissolved at room temperature using a magnetic stirrer, then left for one hour to make sure there are no residues when spraying the solution on the glass substrate. CdO doped with cobalt thin films were obtained from cobalt chloride (CoCl₂), (BDH Chemical England, 99.5% purity), a sky blue powder with good solubility in water. The solution was prepared with a concentration of 0.1M, and 3% and 5% of the solution was added to the cadmium nitrate solution, and then mixed well until becoming homogeneous and clear. In that manner, the cadmium nitrate solution with a specific weight ratio of cobalt chloride was obtained.

The films are deposited on glass substrates (2.5×2.5) cm² after cleaning them thoroughly with water and detergent to ensure that any oil stains or residues of suspended material are removed then washed with distilled water, after that they were immersed in alcohol for 15 minutes in a water bath, then dried by dust cleaner .

$$M = \frac{W_t}{M_{wt}} \left(\frac{1000}{V} \right) \dots \dots \dots 1$$

where M: Molarity of solution.

W_t: Dissolved weight of the compound in the size of 1000 ml (g).

M_{wt}: Molecular weight for the compound cadmium nitrate tetrahydrate (g/mol).

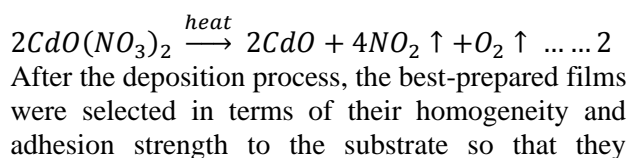
V: Total volume of solution (m³).

After several tests, the most appropriate conditions were chosen in the preparation of the films as shown in Table 1.

Table 1. Selected variables for the preparation of thin films

Nozzle-Substrate Distance	Gas Pressure	Spray Time	Stopping Time	Substrate Temperature	Solution Flow Rate	Carrier Gas	Thickness nm	Molarity
15 ±2 cm	1 Bar	5 sec	12 sec	350 °C	2 ml/s	O ₂	150 ±5	1M

The solution was placed in the container capacity and sprayed on the substrates. The cadmium oxide thin films are obtained through the following chemical reaction:



cannot be cleared by hand and are free from discolored spots, impurities, and cracks in the films. The homogeneity of the films is diagnosed in stages, first with the eye. If none of the above defects are detected using an optical microscope, the crystal structure is examined using a diffraction method with x-rays system (Cu-K α , $\lambda=0.154$ nm, 40 kV, 20 mA. Measurements of the optical properties were performed by using UV-VIS double beam Spectrometer with the range of 200-900 nm.

Structural Analysis XRD characterization

Figure 1 shows the results of XRD analysis for undoped CdO and doped with different concentrations of Co thin films. The figure revealed a polycrystalline nature with cubic structure with diffraction peaks returning to the crystalline plane (111) (200) (202) (311) at 2θ of 26.4°, 32.4°, 52.1° and 64.3°, respectively. This result agrees with articles in (2,10,16). That corresponds well with standard card of data (JCPDS Card No. 96-900-6693) (17). These peaks show a variation in their intensity with a strong, sharp peak toward a plane (111), that is a property possessed by high crystallization material and it is representing the preference for crystalline development, agrees with the results obtained by (16,18). The reason for the preference for film growth at the (111) peak is that the energy of the surface density of this orientation is lower than other crystalline orientations (19). However, by increasing Co concentration, the CdO (111) orientation becomes more prominent. There was an increasing in CdO (111) orientation intensity which indicates an improving crystallinity and increasing the crystallite size (D) as increasing Co concentration. A matching of the calculated d_{hkl} values and the standard ones confirms that the Co doped CdO films at 3% and 5% are also crystallized in the cubic structure.

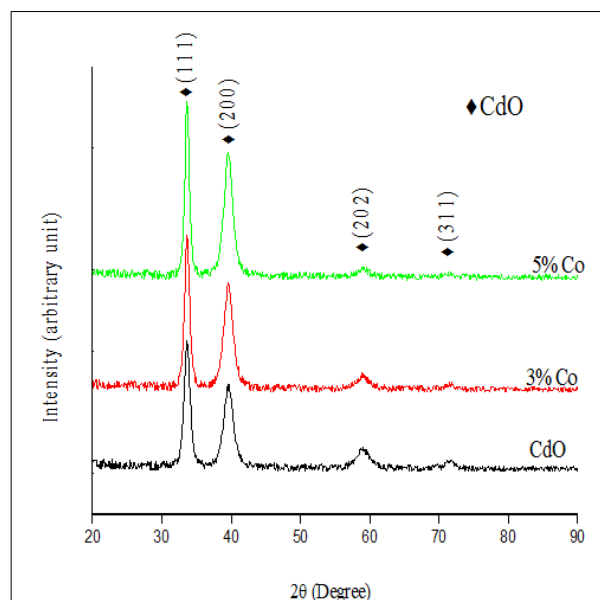


Figure 1. XDR diagram for un-doped and Co doped CdO.

Table 2 shows a decrease in β , which resulted in a rise in the intensity of dominant peaks, consistent with the Ref. (11,20) indicating the improvement in the crystalline growth of the deposited atoms accompanied by an increase in crystallite size with increasing of Co doping concentration, a similar result obtained by the researcher (21). The CdO:Co nanostructure at 5% exhibited a larger crystallite size, it found about 11.1 nm, while it was 8.4 nm and 9.9 nm for undoped and 3% Co-doped respectively, as shown in Table 2. In addition, it was evident that there is a decrease in the values of dislocations with increasing Cobalt concentration. This may be due to the fact that increasing of Co concentration reduce the crystalline defects accompanying the process of crystalline growth.

There was no change in the location of the diffraction peaks at 3% dopant ratio, which indicates stability in the crystalline structure of the prepared films before and after doping at this ratio. Maybe due to the fact that the 3% doping ratio was a diminutive, so does not lead to deforming the crystalline structure. When the dopant ratio reached 5%, there was a small shift in the diffraction peaks towards the low 2θ and thus an increase in the lattice parameter (a) same behavior for CdO when doped with fluorine (21), with an increase in particle size and a decrease in (β).

Table 2. structural parameters of thin films.

Co-Concentration %	2θ (Deg.)	FWHM (Deg.)	d _{hkl} Exp.(Å)	d _{hkl} Std.(Å)	G.S (nm)	hkl	a (Å)	δ × 10 ¹² lines/m ²	Phase
Pure	33.6354	0.9938	2.6624	2.6683	8.4	111	4.61138	1.40	CdO
	39.5981	1.5901	2.2741	2.3108	5.3	200	3.93892	3.50	CdO
	58.9770	2.1863	1.5649	1.634	4.2	202	2.71042	5.70	CdO
	71.4988	1.6894	1.3185	1.3935	5.8	311	2.28364	3.00	CdO
3%	33.6354	0.8400	2.6624	2.6683	9.9	111	4.61138	1.00	CdO
	39.5981	1.5444	2.2741	2.3108	5.5	200	3.93892	3.30	CdO
	58.9770	1.9502	1.5649	1.634	4.7	202	2.71042	4.60	CdO
	71.4988	1.5700	1.3185	1.3935	6.2	311	2.28364	2.60	CdO
5%	33.6304	0.7490	2.6628	2.6683	11.1	111	4.61204	0.81	CdO
	39.5931	1.4664	2.2744	2.3108	5.8	200	3.93939	3.00	CdO
	58.9720	1.7442	1.5650	1.634	5.2	202	2.71062	3.60	CdO
	71.4938	1.4720	1.3185	1.3935	6.7	311	2.28378	2.30	CdO

Atomic Force Microscopy (AFM):

Surface distribution of atoms on glass substrates was studied using an atomic force microscope for un-doped CdO and doped with 3 and 5% Co. Figure 2 shows the density of grain distribution and three-dimensional images. It reveals a homogeneous distribution of the clusters, noting that the process of growth of atoms was regular and the deposition process was successful. The parameters of the AFM have been listed in Table 3. A study of surface characteristics showed that the particle size of the films under study increased by increasing the Co-concentration, which is consistent with the results of the study of X-ray diffraction. In addition, there was an increase in the

roughness of the surface with increasing dopant concentration, may be attributed to the increase in particle size with increasing Co-doping (22).

Table 3. Variation of average diameter and roughness as a function to the dopant concentration

Type	Average diameter (nm)	Average roughness (nm)	r.m.s roughness (nm)
Pure	22	1.03	1.22
3% Co	28	1.44	1.65
5% Co	40	2.59	3

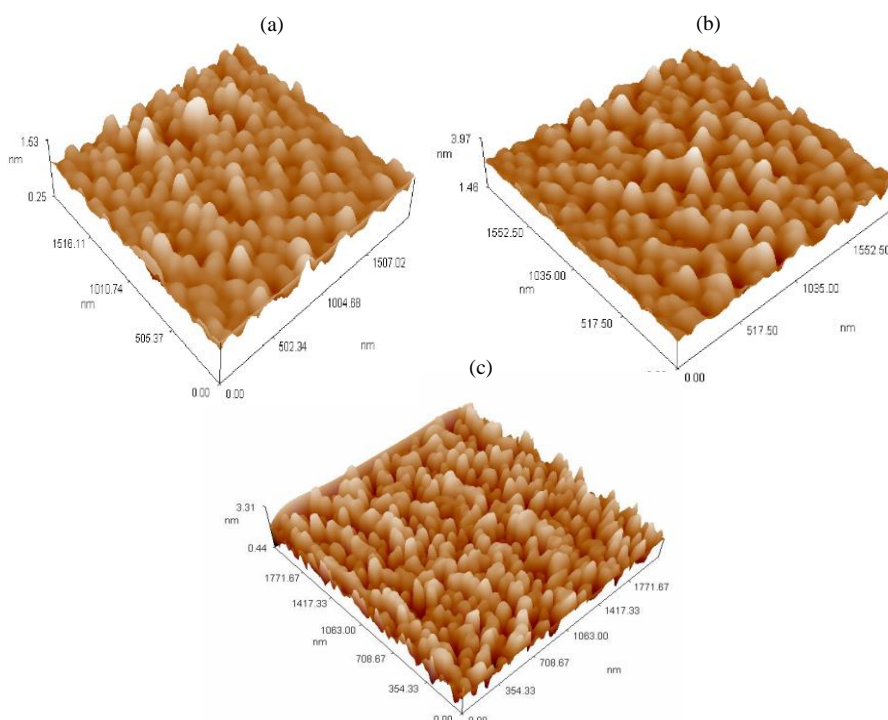


Figure 2. AFM images for; (a) un-doped CdO, (b) doped with 3% Co, and (c) doped with 5% Co thin films.

Optical Properties:

Transmittance (T%):

Figure 3 shows transmittance spectrum of prepared films within the range 300-1100 nm of wavelength, undoped samples reported higher values of transmittance in UV-visible range towards IR of the electromagnetic spectrum, higher than 85%, agrees with ref. (23), therefore these films can be used in the field of optical windows applications. The films showed similar behavior for all optical analysis, which gives an impression of their stability. However, after doping with different concentrations of cobalt, there was an inversely related between T% and doping concentration. Undoped film has 78.25% of transmittance as the average value while decreased to 74.83% and 69.93% for 3% and 5% Co-doped films respectively. This decrease in T% after the doping can be attributed to the increase in crystallite size, as shown in XRD analysis, which refers to an increase in absorbance (A) vs. doping

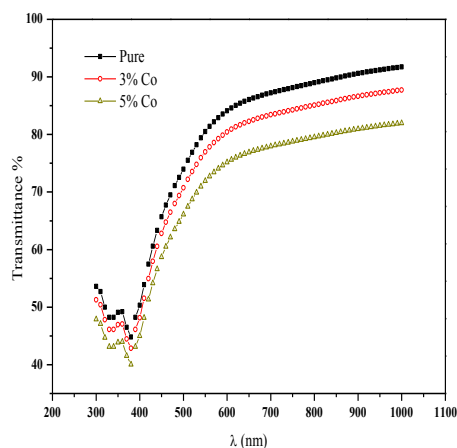


Figure 3. Transmittance as a function to the wavelength of un-doped CdO and doped with different concentrations of Co.

Absorption Coefficient (α):

Figure 5 shows the absorption coefficient curve, which reveals increasing in its values with a decrease in wavelength. As mentioned in the discussion section of optical transmittance, there was a decrease in absorbance towards increasing wavelength leads to a decrease in absorption coefficient (α) because of both absorbance and the absorption coefficient linked by low of lambert, the relation 4:(25)

$$\alpha = 2.303 \frac{A}{t} \dots \dots \dots 4$$

t: Film thickness.

While there was an increase in α accompanied by a drag out in the absorption edge towards higher λ with increasing of Co-dopant concentration, as shown in Table 5, which gives us an indication of a decrease in energy gap values, as will be discussed

concentration. Table 4 shows the transmittance at the absorption edges (T_{edge}), at the middle of spectrum (T_{middle}), the maximum transmittance (T_{maximum}), and the average transmittance (T_{average}). As well as the optical measurements revealed decreasing in absorbance vs wavelength, as shown in Fig.4, within the measured wavelength range according to the relation 3 :(24)

$$T = e^{-2.303 A} \dots \dots \dots 3$$

T: transmittance and A: absorbance.

Table 4. The Transmittance at the absorption edges, middle of spectrum, the maximum transmittance, and the average transmittance.

Cobalt concentration %	T _{edge} %	T _{middle} %	T _{maximum} %	T _{average} %
0	44.80	80.49	91.72	78.25
3	42.84	76.97	87.71	74.83
5	40.04	71.93	81.97	69.93

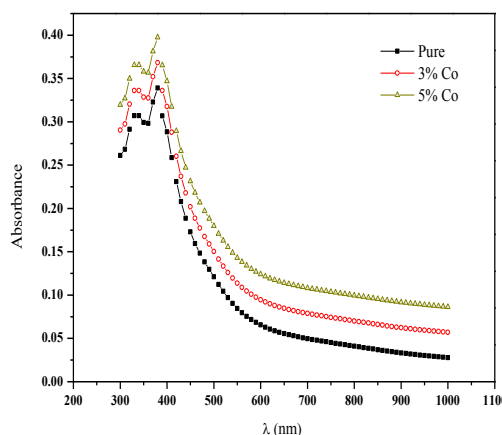


Figure 4. Absorbance as a function to the wavelength of un-doped CdO and doped with different concentrations of Co.

later. This may be due to the doping that resulted in the generation of donor energy levels within the energy gap near the conduction band, which in turn led to the absorption of low-energy photons and thus a clear increase in absorption factor values (26). Figure 5 shows also higher values for α rather than 10⁴, this may be indicative of direct electronic transitions between the valence and conduction bands, which may be attributed to an increase in the absorption values within this region.

Table 5. The absorption coefficient at the absorption edges (α_{edge}), middle of spectrum (α_{middle}), the maximum absorption coefficient ($\alpha_{maximum}$), and the average value ($\alpha_{average}$).

Cobalt concentration %	α_{edge} ($\text{cm}^{-1} \times 10^4$)	α_{middle} ($\text{cm}^{-1} \times 10^4$)	$\alpha_{maximum}$ ($\text{cm}^{-1} \times 10^4$)	$\alpha_{average}$ ($\text{cm}^{-1} \times 10^4$)
0	3.90	0.97	0.32	1.23
3	4.24	1.31	0.66	1.56
5	4.58	1.65	0.99	1.90

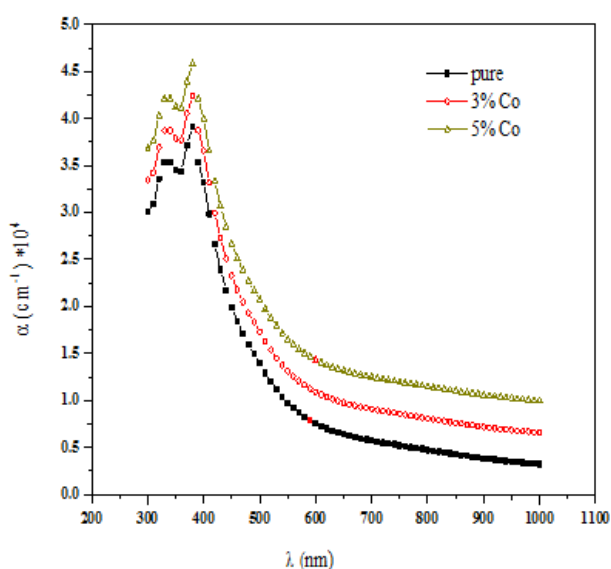


Figure 5. Absorption coefficient vs wavelength for CdO and Co:CdO thin films.

Energy Gap (E_g):

The optical energy gap values for direct electronic transition of both types allowed and unallowed are calculated through the relation 5: (27)

$$\alpha h\nu = A ((h\nu) - E_g)^n \dots \dots \dots 5$$

A: constant depends on the structure of material and if the electronic transition from the allowed direct type, then (n) will be taking the value $(\frac{1}{2})$, while (n) will be taking the value (2) for the allowed indirect transition (28). Figure 6a shows the optical energy gap values for allowed direct transition (ADT) which have the values 2.78, 2.7 and 2.63 eV for un-doped CdO and doped with 3% and 5% Co thin films respectively. The results agreeing with reported literature (2,16,29). These values are confirming the formation of nanostructures thin films (30). Also means that the absorption of photons was direct, but the breadth of absorption region indicates that there were different types of absorption, indirect or by the tails of localized levels inside the energy gap that arose from the change in the crystal structure obtained by adding Co to the alloy. The absorption edge shifted from 380 nm toward the infrared as Co content increased.

At 3%, the absorption edge appeared at 389 nm, while at 5% the absorption edge was at 392 nm. The change in the energy gap can be the reason for the increase in particle size with the increase in the doping concentration (31). Figure 6b shows the change in values of the energy gap and particle size as a function of doping concentration depending on the values listed in Table 6. The graph in Fig.6c shows the plot of $(\alpha h\nu)^{\frac{1}{2}}$ vs photon energy for the allowed indirect transition (AIDT), which has the values 1.85, 1.7 and 1.55 eV for pristine CdO, 3% Co doped, and 5% Co doped, respectively.

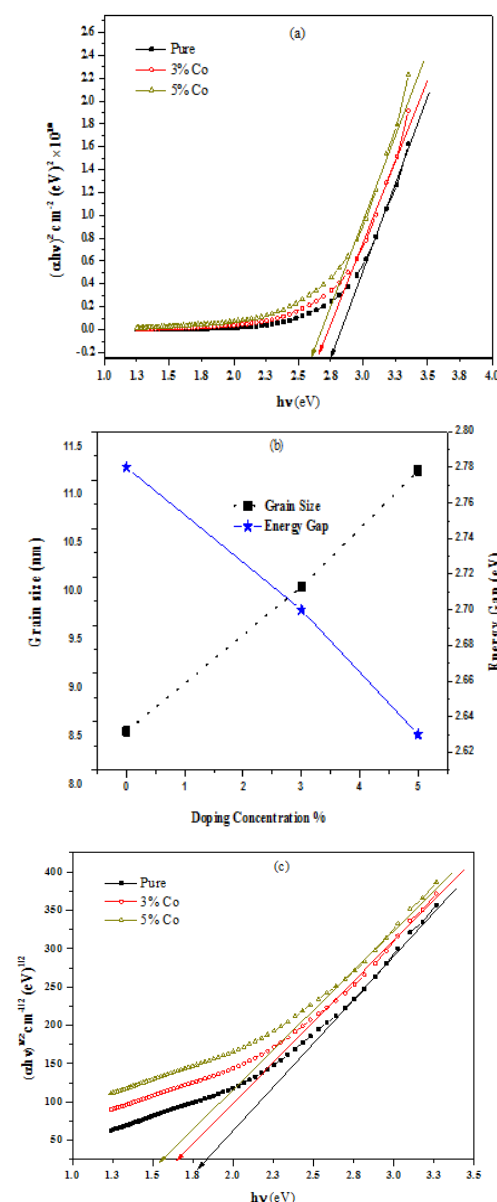


Figure 6. a- Energy gap with photon energy for the allowed direct transition, b- Particle size and E_g vs doping concentration, c- Energy gap with photon energy for the allowed indirect transition.

Table 6. Relation between grain size and optical energy gap according to Co-dopant variation.

Type	G.S (nm)	E_g (ADT)eV	E_g (AIDT)eV
Pure	8.4	2.78	1.85
3% Co	9.9	2.7	1.7
5% Co	11.1	2.63	1.55

Conclusions:

Undoped and Cobalt doped CdO thin films are successfully synthesized by (SPT) on glass substrate. Co doping of CdO leads to increasing surface roughness and energy bandgap. The increase in bandgap could lead to a decrease in electrical conductivity. Therefore, Co doping is not recommended in transparent conductive oxides applications but it can work as a window in some other applications. The increase in grain size diameter can approve that Co is encouraging certain orientations growth and introducing thin films with better quality. Finally, the surface roughness increases with increased cobalt ratios, and this contributes greatly to the advantage of using these ratios in gas sensor devices.

Authors' declaration:

- Conflicts of Interest: None.
- We hereby confirm that all the Figures and Tables in the manuscript are mine ours. Besides, the Figures and images, which are not mine ours, have been given the permission for re-publication attached with the manuscript.
- Ethical Clearance: The project was approved by the local ethical committee in University of Anbar.

References:

1. Benhamida S, Benhaoua B, Barir R, Rahal A, Benhaoua A. Effect of sprayed solution volume on structural and optical properties of nickel oxide thin films. *J Nano- Electron Phys.* 2017; 9(3):1–5.
2. Maragatham V, Sushmitha V, Deepak Raj P, Sridharan M. Studies on sputtered ZnO:CdO thin films for TCO application. *IOP Conf Ser Mater Sci Eng.* 2018; 310(1):1–6.
3. Martin EJJ, Yan M, Lane M, Ireland J, Kannewurf CR, Chang RPH. Properties of multilayer transparent conducting oxide films. *Thin solid Film.* 2004; 461(2):309–15.
4. Jeong W J, Park G C. Electrical and optical properties of ZnO thin film as a function of deposition parameters. *Sol Energ Mat Sol C.* 2001; 65(1):37–45.
5. Stadler A. Transparent Conducting Oxides—An Up-To-Date Overview. *Materials (Basel).* 2012; 5(12):661–83.
6. Edwards PP, Porch A, Jones MO, Morgan D V, Perks RM. Basic materials physics of transparent conducting oxides. *Dalton Trans.* 2004 ;(19):2995–3002.
7. Chopra KL, Major S, Pandya DK. Transparent conductors-A status review. *Thin Solid Films.* 1983; 102(1):1–46.
8. Kawazoe H, Ueda K. Transparent Conducting Oxides Based on the Spinel Structure. *J Am Ceram Soc.* 2004; 82(12):3330–6.
9. Soonmin H. Synthesis and Properties of Cadmium Oxide Thin Films: a Review. *Int J Curr Adv Res.* 2016;5(7):3–7.
10. Kavitha B, Nirmala M, Poornachandra S, Pavithra M. Preparation and Characterization of CdO Thin Films Prepared by Chemical Method. *J Environ Nanotechnol.* 2017; 6(1):59–66.
11. Das MR, Mukherjee A, Mitra P. Structural, optical and electrical characterization of CBD synthesized CdO thin films: Influence of deposition time. *Mater Sci-Poland.* 2017; 35(3):470–8.
12. Shehab AA, Mahmoud T H. Study the Influence of Sn Dopant on the Some Structural and Optical Properties of Pure Cadmium Oxide (CdO) Thin Films. *Ibn Al-Haitham J Pure Appl Sci.* 2012; 25(2):170–82.
13. Dhivya P, Prasad AK, Sridharan M. Nanostructured cadmium oxide thin films for hydrogen sensor. *Int J Hydrog Energ.* 2012; 37(23):18575–8.
14. Uplane MD, Kshirsagar PN, Lokhande BJ, Lokhande CD. Preparation of cadmium oxide films by spray pyrolysis and its conversion into cadmium chalcogenide films. *Indian J Pure Ap Phy.* 1999; 37(8):616–9.
15. Quiñones-Galván JG, Lozada-Morales R, Jiménez-Sandoval S, Camps E, Castrejón-Sánchez VH, Campos-González E, et al. Physical properties of a non-transparent cadmium oxide thick film deposited at low fluence by pulsed laser deposition. *Mater Res Bull.* 2016; 76:376–83.
16. Ghdeeb N J. Effect of Molar Concentration on Structural, Morphological and Optical Properties of CdO Thin Films Prepared by Chemical Spray Pyrolysis Methode. *Int J Sci Res.* 2017; 6(2):1351–4.
17. Zhang J. Room-temperature compressibilities of MnO and CdO: further examination of the role of cation type in bulk modulus systematics. *Phys Chem Miner.* 1999; 26(8):644–8.
18. Kathalingam A, Kesavan K, Sarwar H, Jeon J, Kim H. Analysis of Sn Concentration Effect on Morphological, Optical, Electrical and Photonic Properties of Spray-Coated Sn-Doped CdO Thin Films. *Coating.* 2018; 8(167):1–15.
19. Ismail RA, Ghafari S, Sihat RS. Characteristics study of nanostructured CdO prepared by spray pyrolysis. *Int Lett Chem Phys Astron.* 2015; 53:165–72.
20. Mahasen MM, Soraya MM, Yousef EL S, GOMAA A M, Shaaban ER. Structural, thermal and optical analyses of cobalt-doped cdo thin films. *J Ovonic Res.* 2019; 15(4):247–60.
21. Badera N, Godbole B, Srivastava SB, Vishwakarma PN, Deepti J, sharath L S, et al. Photoconductivity of

- Cobalt doped CdS thin films. Phys Procedia. 2013; 49:190–8.
22. Iftikar M A, Rzaij J M, Abbas QA, Ibrahim IM, Alatta HJ. Structural, Optical and Sensing Behavior of Neodymium-Doped Vanadium Pentoxide Thin Films. Iran J Sci Technol A. 2018; 42(4):2375–2386.
23. Umeokwonna NS, Ekpunobi AJ, Ekwo PI. Effects of Cobalt Doping on the Optical Properties of Cadmium Cobalt Oxide Nanofilms Deposited by Electrodeposition Method. Int J Eng Res 2015; 6(7):504–13.
24. Ibraheam AS, Rzaij J M, Fakhri M, Abdulwahhab A W. Structural, optical and electrical investigations of Al:ZnO nanostructures as UV photodetector synthesized by spray pyrolysis technique. Mater Res Express. 2019; 6(5).
25. Aishwarya V N, Nirmala D N, Jeyaprakash B G, Chandiramouli R. Preparation and Characterization of Highly Conducting and Optically Transparent Fluorine Doped CdO Thin Films. J Appl Sci. 2012; 12(16):1630–5.
26. Ali O M. Elementary solid state physics : principles and applications. Addison-Wesley Publ Company, First Prin. 1975.
27. Rzaij J M, Ibrahim I M, Alalouisi M A, Habubi N F. Hydrogen sulfide sensor based on cupric oxide thin films. Optik. 2018; 172:117–26.
28. Usharani K, Raja N, Manjula N, Nagarethinam VS, Balu AR. Characteristic Analysis on the Suitability of CdO Thin Films towards Optical Device Applications – Substrate Temperature Effect. Int J Thin Film Sci Tec. 2015; 4(89):89–96.
29. Kumar S, Singh F, Kapoor A. Study of valence band tailing effect induced by electronic excitations in nanocrystalline cadmium oxide thin films. Optik. 2016; 127(4):2055–8.
30. Haoshuang Gu, Zhao W, Yongming Hu. Hydrogen Gas Sensors Based on Semiconductor Oxide Nanostructures. Sensors. 2012; 12(5):5517.
31. Thambidurai M, Muthukumarasamy N, Velauthapillai D. Effect of Cr-doping on the structural and optical properties of CdS nanoparticles prepared by chemical precipitation method. J Mater. 2012; 4(4):1–5.

تأثير الكوبالت على نمو التركيب النانوي من أكسيد الكاديوم المحضر بتقنية التحلل الكيميائي الحراري

امينة محسن عباس³

عثمان سالم ابراهيم²

جمال مال الله رزيج¹

¹قسم الفيزياء، كلية العلوم، جامعة الانبار، الرمادي، العراق
²وزارة التربية العراقية، الانبار، العراق
³قسم الكيمياء، كلية العلوم، جامعة النهرين، بغداد، العراق

الخلاصة:

تم استخدام تقنية الرش الكيميائي الحراري (SPT) للحصول على تركيب نانوي من اغشية اوكسيد الكاديوم المشوبة بالكوبالت بنسبة 3% و5%. تم ترسيب الأفلام على قواعد من الزجاج بدرجة حرارة 350 درجة مئوية وبسمك 150 نانومتر. أظهرت نتائج حيود الاشعة السينية (XRD) بنية بلورية متعددة التبلور ذات تركيب مكعبي بأفضلية إمام بلوري باتجاه المستوي (111). اشتملت فحوصات الاشعة السينية أيضا دراسة المسافة البينية بين المستويات البلورية والحجم البلوري وثوابت الشبكة وكثافة الانخلاعات البلورية. سطوح متجانسة وتوزيع منتظم للذرات اظهرتها صور مجهر القوى الذرية (AFM) بمعدل خشونة للسطح بمقدار 1.3 نانومتر ومتوسط جذر تربيعي للخشونة بمقدار 1.22 نانومتر. كشفت دراسة الخواص البصرية ان الأفلام المحضرة تمتلك نفاذية بصرية أكبر من 85% في مدى الطيف المرئي وتقل قيمتها مع زيادة نسب التشويب بالكوبالت. تناقص في قيم معامل الامتصاص مع زيادة الطول الموجي وان الاغشية المحضرة تمتلك قيم معامل امتصاص أكبر من 10⁴ سم⁻¹. تراوحت قيم فجوة الطاقة البصرية للانتقال المباشر المسموح من 2.78 إلى 2.63 إلكترون فولت مع زيادة تركيز الكوبالت، في حين تراوحت قيم فجوة الطاقة للانتقال غير المباشر المسموح من 1.85 إلى 1.6 إلكترون فولت.

الكلمات المفتاحية: أكسيد الكاديوم، كوبالت، الخصائص البصرية، الرش الكيميائي، أغشية رقيقة.